Aromatic Interactions Are Not Required for Amyloid Fibril Formation by Islet Amyloid Polypeptide but Do Influence the Rate of Fibril Formation and Fibril Morphology†

Peter Marek,‡ Andisheh Abedini,‡ BenBen Song,‡ Mandakini Kanungo,§ Megan E. Johnson,‡ Ruchi Gupta,‡ Warda Zaman,‡ Stanislaus S. Wong,‡,§ and Daniel P. Raleigh*,‡,||

Department of Chemistry, State University of New York, Stony Brook, New York 1179-3400, Condensed Matter Physics and Materials Science Department, Brookhaven National Laboratory, Building 480, Upton, New York 11973, Graduate Program in Biophysics, State University of New York, Stony Brook, New York 11794, and Graduate Program in Biochemistry and Structural Biology, State University of New York, Stony Brook, New York 11794

Received October 23, 2006; Revised Manuscript Received December 14, 2006

ABSTRACT: Amyloid formation has been implicated in a wide range of human diseases, and a diverse set of proteins is involved. There is considerable interest in elucidating the interactions which lead to amyloid formation and which contribute to amyloid fibril stability. Recent attention has been focused upon the potential role of aromatic−aromatic and aromatic−hydrophobic interactions in amyloid formation by short to midsized polypeptides. Here we examine whether aromatic residues are necessary for amyloid formation by islet amyloid polypeptide (IAPP). IAPP is responsible for the formation of islet amyloid in type II diabetes which is thought to play a role in the pathology of the disease. IAPP is 37 residues in length and contains three aromatic residues, Phe-15, Phe-23, and Tyr-37. Structural models of IAPP amyloid fibrils postulate that Tyr-37 is near one of the phenylalanine residues, and it is known that Tyr-37 interacts with one of the phenylalanines during fibrillization; however, it is not known if aromatic−aromatic or aromatic−hydrophobic interactions are absolutely required for amyloid formation. An F15L/F23L/Y37L triple mutant (IAPP-3XL) was prepared, and its ability to form amyloid was tested. CD, thioflavin binding assays, AFM, and TEM measurements all show that the triple leucine mutant readily forms amyloid fibrils. The substitutions do, however, decrease the rate of fibril formation and alter the tendency of fibrils to aggregate. Thus, while aromatic residues are not an absolute requirement for amyloid formation by IAPP, they do play a role in the fibril assembly process.

Amyloid formation plays a role in a wide range of human diseases, including Alzheimer's disease and type II diabetes, and a diverse set of proteins has been shown to form amyloid in vivo and in vitro. There has been considerable interest in determining the factors and specific interactions which lead to amyloid formation (*1*−*10*). Recent attention has been focused on the potential role of aromatic−aromatic and aromatic−hydrophobic interactions in amyloid formation (*1*−*3*, *5*, *6*, *11*−*13*). Aromatic−aromatic interactions are known to contribute to the stability of globular proteins and have been suggested to play a critical role in amyloid formation (*11*, *12*). Initial experiments involving alanine scanning of peptides containing a single aromatic residue seemed to support this conjecture (*12*). In particular, substitution of aromatic residues in short peptides derived from islet amyloid polypeptide (IAPP,[1] amylin) by alanine significantly inhibited amyloid formation or abolished it. Alanine is, however, a nonconservative substitution for phenylalanine, particularly with regard to amyloid formation since it is smaller and less hydrophobic and has a lower β-sheet propensity. Indeed, substitution of aromatic residues with leucine instead of alanine led to peptides which still formed amyloid (*13*). These studies were performed on short fragments derived from IAPP or from other proteins. IAPP contains multiple aromatic residues, and intrapeptide aromatic−aromatic interactions occur during the fibrillization process; however, it is not known if these intrapeptide aromatic−aromatic interactions are strictly required for amyloid formation by intact IAPP (*14*). The question is important because amyloid formation by IAPP is potentially of great medical signifi-

† A.A. was supported by a GAANN fellowship from the Department of Education. M.E.J. was an REU summer student supported by the Stony Brook NSF REU program. The work was supported in part by grants from the National Institutes of Health (Grant GM70941 to D.P.R.) and the National Science Foundation (Grant DMR-0348239 to S.S.W.).

* To whom correspondence should be addressed: State University of New York, Stony Brook, NY 11794. Telephone: (631) 632-9547. Fax (631): 632-7960. E-mail: draleigh@notes.cc.sunysb.edu.

‡ Department of Chemistry, State University of New York.

§ Brookhaven National Laboratory.

|| Graduate Program in Biophysics and Graduate Program in Biochemistry and Structural Biology, State University of New York.

[1] Abbreviations: AFM, atomic force microscopy; CD, circular dichroism; DMSO, dimethyl sulfoxide; Fmoc, 9-fluorenylmethoxycarbonyl; HPLC, high-performance liquid chromatography; IAPP, islet amyloid polypeptide; IAPP-3XL, F15L/F23L/Y37L triple mutant of IAPP; MALDI-TOF MS, matrix-assisted laser desorption ionization time-of-flight mass spectrometry; PAL-PEG, 5-(4′-Fmoc-aminomethyl-3′,5-dimethoxyphenol)valeric acid; TEM, transmission electron microscopy; TFA, trifluoroacetic acid; v/v, volume to volume.

10.1021/bi0621967 CCC: $37.00
Published on Web 02/21/2007

cance, and there have been suggestions that targeting aromatic−aromatic interactions is a viable strategy for the design of amyloid inhibitors, particularly for IAPP (*15*, *16*).

IAPP is a hormone which is stored in the insulin secretory granules and is cosecreted with insulin (*17*, *18*). In its normal soluble state, it plays a role in regulating glucose metabolism, but in type II diabetes, IAPP forms amyloid deposits in the pancreas (*17*−*23*). Islet amyloid is believed to play a role in the pathology of type II diabetes, and more than 90% of patients with type II diabetes exhibit islet amyloid upon autopsy (*23*). Furthermore, the level of islet amyloid appears to correlate with the severity of the disease. The mature form of IAPP is 37 residues in length, has an amidated C-terminus, and contains a disulfide bridge between residues 2 and 7 (*17*, *18*). The human form of the polypeptide contains three aromatic residues, Phe-15, Phe-23, and Tyr-37. FRET studies have shown that the C-terminal Tyr interacts with one or more of the Phe residues during the fibrillization process (*14*). FRET studies have also shown that Tyr-37 is relatively immobile in the final fibril structure, while structural models of the fibrils suggest that Tyr-37 could form aromatic−aromatic interactions with Phe-23 (*14*, *24*). These studies indicate that aromatic residues may be important in formation of amyloid by the full-length peptide. Note that the studies with short peptides described above could not test the importance of these interactions because each peptide contained only one aromatic residue; thus, intrapeptide aromatic−aromatic interactions were not possible.

A number of studies have suggested that targeting aromatic−aromatic interactions is a viable strategy for the design of amyloid inhibitors, particularly of IAPP (*15*, *16*, *25*). However, no studies have been reported which test if aromatic−aromatic or aromatic−hydrophobic interactions are absolutely necessary for islet amyloid formation. The question is important, both because of the growing interest in inhibitors of IAPP aggregation and because of the general insight such a study might offer into amyloid formation in a broader context. Here we report the characterization of a triple mutant of IAPP in which all three aromatic residues are replaced with Leu. The peptide is denoted IAPP-3XL, and as described below, it readily forms amyloid. Thus, aromatic residues are not required for amyloid formation by IAPP, although amyloid formation is slower in their absence and the final morphology is subtly affected.

EXPERIMENTAL PROCEDURES

Peptide Synthesis and Purification. IAPP-3XL was synthesized on a 0.25 mmol scale with an Applied Biosystems 433A peptide synthesizer utilizing 9-fluorenylmethoxycarbonyl (Fmoc) chemistry. Solvents that were used were ACS-grade. Fmoc-protected pseudoproline (oxazolidine) dipeptide derivatives were used as previously described (*26*). They were purchased from Novabiochem. All other reagents were purchased from Advanced Chemtech, PE Biosystems, Sigma, and Fisher Scientific. Use of a 5-(4′-Fmoc-aminomethyl-3′,5-dimethoxyphenol) valeric acid (PAL-PEG) resin afforded an amidated C-terminus. Standard Fmoc reaction cycles were used. The first residue attached to the resin, all β-branched residues, the residue directly following a β-branched residue, all psuedoproline dipeptide derivatives, and the residue directly following a pseudoproline dipeptide derivative were double-coupled. The peptide was cleaved from the resin through the use of standard trifluoroacetic acid (TFA) methods.

Peptide Purification. The crude peptide (100 mg) was dissolved in 10% acetic acid (v/v), frozen in liquid nitrogen, and lyophilized to increase its solubility. The dry polypeptide was dissolved in 5 mL of DMSO to promote the formation of the Cys-2−Cys-7 disulfide bond (*27*). After 24 h, the solution was purified via reverse-phase high-performance liquid chromatography (RP-HPLC) using a Vydac C18 preparative column. A two-buffer system was utilized in which buffer A consisted of H_2O and 0.045% HCl (v/v) and buffer B consisted of 80% acetonitrile, 20% H_2O, and 0.045% HCl (v/v). The identity of the pure polypeptide was confirmed by matrix-assisted laser desorption ionization time-of-flight mass spectrometry (MALDI-TOF MS). The purity of the polypeptide was checked by HPLC using a Vydac C18 analytical column.

Thioflavin-T Fluorescence Assays. A 0.53 mM peptide stock solution consisting of 1.9 mg of purified IAPP-3XL in 1 mL of 20 mM Tris-HCl buffer (pH 7.4) was prepared and allowed to incubate for 2 days at room temperature. A second 0.53 mM peptide stock solution was prepared on the second day and used to monitor events at time zero. Fluorescence was measured on a Jobin Yvon Horiba fluorescence spectrophotometer with excitation at 450 nm and emission at 485 nm. The emission and excitation slits were set to 5 nm, and a 1.0 cm cuvette was used. The wavelength scan was measured from 462 to 650 nm. All thioflavin-T fluorescence experiments were performed by diluting 103 μL of the stock solution into a 20 mM Tris-HCl buffer (pH 7.4) containing thioflavin-T. The final solution conditions were 32 μM peptide and 32 μM thioflavin-T at pH 7.4. All solutions were stirred during the wavelength scans to maintain solution homogeneity. As a control, a fluorescence spectrum was taken of a solution consisting of only buffer and thioflavin-T. This spectrum was flat in comparison to the spectrum of the solution containing the peptide, indicating that the fluorescence observed in the presence of the peptide is due to the peptide fibril−dye interactions. The background spectrum was subtracted from the spectra of the peptide samples. Wavelength scans were performed on both peptide stock solutions on the day of preparation and after incubation for 15 days. Studies were also conducted in which a 1.58 mM stock solution was prepared in 100% HFIP as described previously (*27*). These conditions are used to ensure that IAPP is monomeric at the initiation of the kinetic assays. Kinetic studies were performed by diluting this stock solution by a factor of 50:1 in Tris-HCl buffer (pH 7.4) containing thioflavin-T and monitoring the thioflavin fluorescence as a function of time. Final solution conditions were 32 μM IAPP and 32 μM thioflavin-T (pH 7.4) with 2% HFIP (v/v). The kinetics of amyloid formation by IAPP are dependent on the size and shape of the cell that is used, the sample volume, and whether samples are stirred as well as the solvent composition.

Circular Dichroism. Far-UV CD experiments were performed at 25 °C on an Aviv 62A DS CD spectrophotometer. For far-UV CD wavelength scans, an aliquot from the peptide stock was diluted into 20 mM Tris-HCl buffer (pH 7.4), for a total volume of 250 μL. The final peptide concentration was 0.1 mg/mL in 20 mM Tris-HCl buffer. The spectrum is

(A) **Wild-type hIAPP**

1	10	20	30	37
KCNTATCAT	QRLAN**F**LVHS	SNN**F**GAILSS	TNVGSNT**Y**	

(B) **hIAPP-3XL**

1	10	20	30	37
KCNTATCAT	QRLAN**L**LVHS	SNN**L**GAILSS	TNVGSNT**L**	

FIGURE 1: Primary sequence of (A) wild-type human IAPP and (B) the F15L/F23L/Y37L triple mutant. The peptides have an amidated C-terminus, a free N-terminus, and a disulfide bridge between Cys-2 and Cys-7. Positions 15, 23, and 37 are highlighted in bold.

the average of three repeats in a 0.1 cm quartz cuvette and was recorded over a range of 190−250 nm, at 1 nm intervals with an averaging time of 3 s per scan. A background spectrum was subtracted from the collected data.

Transmission Electron Microscopy (TEM). TEM was performed at the University Microscopy Imaging Center at the State University of New York (Stony Brook, NY). Samples (4 μL) from both the $t = 0$ and $t = 2$ days peptide stock solutions were placed on a carbon-coated 300-mesh copper grid and negatively stained with 2% uranyl acetate.

Atomic Force Microscopy (AFM). The peptide samples were characterized using a Nanoscope IIIa Multimode atomic force microscope (Veeco, Inc., Santa Barbara, CA). Specifically, 1 μL of the peptide solution was diluted to 5 μL with deionized water in an Eppendorf tube and mixed gently for 10 s. A 2 μL aliquot of the diluted solution was spin coated onto a freshly cleaved mica surface at 3000 rpm for 30 s followed by air drying for 30 min. The samples were subsequently imaged in ambient air using tapping mode scanning with conventional etched silicon Nanoprobes (k = 3−6 N/m). We used an E scanner for our imaging, with typical scan ranges of <1−5 μm. The scan rate for imaging of the peptides was between 1 and 1.6 Hz; the tapping frequency was between 60 and 90 kHz. The height, length, and periodicity data on the fibrils were obtained directly from flattened images using the as-provided Nanoscope data analysis software. Height, length, and periodicity measurements were taken along a number of line profiles across randomly selected fibrillar features, with our measurements replicated over several images and taken above the mica background. Width measurements were not obtained due to nontrivial tip broadening effects that rendered the data less meaningful.

RESULTS AND DISCUSSION

A triple mutant of human IAPP was synthesized in which each of the aromatic residues was replaced with Leu (F15L, F23L, and Y37L). The polypeptide is denoted IAPP-3XL (Figure 1). Leucine substitutions were used to eliminate the aromatic interactions instead of Ala since Leu is more conservative in terms of its size, hydrophobicity, and β-sheet and α-helical propensity (*13*). The ability of IAPP-3XL to form amyloid was first tested using thioflavin-T binding studies. Thioflavin-T is negligibly fluorescent in solution but experiences a significant increase in quantum yield upon binding to amyloid fibrils. The results indicate that thioflavin-T fluorescence is considerably enhanced in the presence of aggregated IAPP-3XL, exhibiting the characteristic emission maximum near 480 nm associated with the amyloid-bound dye (Figure 2). These studies were conducted using samples prepared in aqueous buffer at relatively high initial concentrations (stock solution was 0.53 mM prior to dilution) as described in Experimental Procedures. We also tested solutions that were first solubilized in 100% HFIP to remove any preformed seeds. Samples prepared by diluting HFIP stock solutions into aqueous buffer also show the characteristic thioflavin-T fluorescence associated with amyloid formation after a short lag phase. This experiment confirms that the positive thioflavin assay is not an artifact of the method of sample preparation. These results were confirmed by far-UV CD studies. Far-UV CD spectra of the triple leucine mutant show the classic conformational transition for amyloid formation by wild-type IAPP, shifting from a random coil structure at time zero to a β-sheet structure (Figure 3).

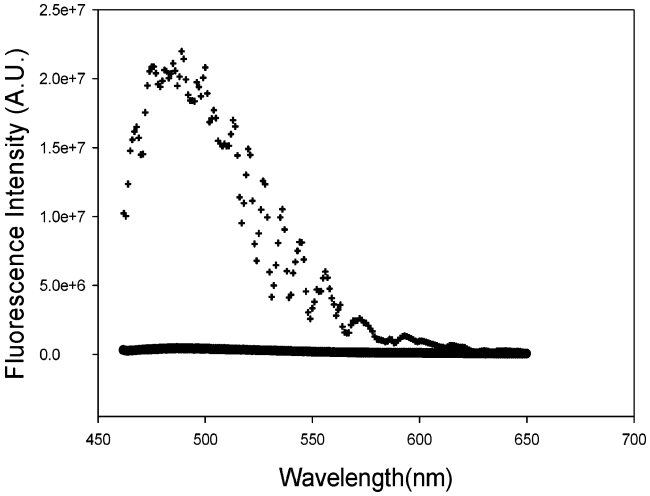

FIGURE 2: Thioflavin-T binds to IAPP-3XL. The solid curve is the thioflavin-T emission spectrum recorded in the presence of 0.53 mM IAPP-3XL which had been incubated for 2 days. The dashed line represents the spectrum of thioflavin-T in buffer in the absence of peptide. Spectra were recorded at 25 °C in 20 mM Tris-HCl (pH 7.4).

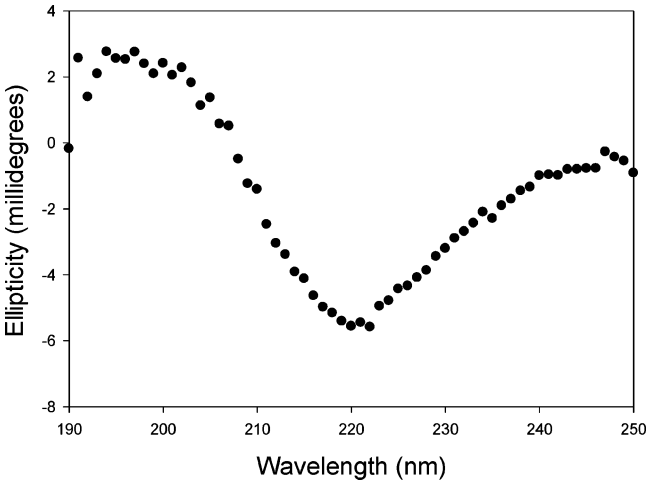

FIGURE 3: IAPP-3XL deposits are rich in β-sheet structure. Far-UV CD spectrum of a 32 μM sample of IAPP-3XL in 20 mM Tris-HCl (pH 7.4).

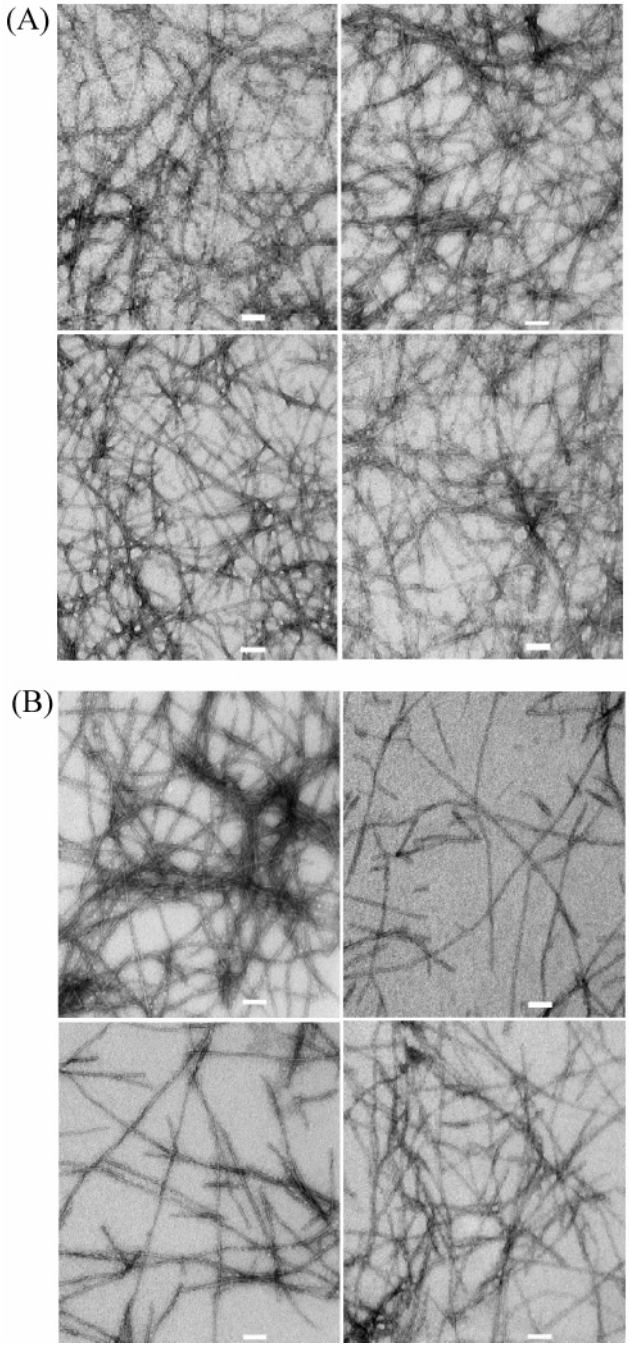

FIGURE 4: IAPP-3XL forms amyloid deposits. (A) TEM images of a sample which had been incubated for 1 h at 25 °C in 20 mM Tris-HCl (pH 7.4). (B) TEM images of samples incubated for 2 days under otherwise identical conditions. The scale bar represents 100 nm.

The morphology of the IAPP-3XL deposits was investigated using TEM. These experiments demonstrate that the material which binds thioflavin-T has the morphology commonly associated with amyloid fibrils. This is an important additional observation because there has been some speculation that thioflavin-T binding can yield false positives. Dense mats of long, unbranched fibrils were observed in the TEM images of samples of IAPP-3XL, which had been incubated for only 1 h at pH 7.4 (Figure 4). Interestingly, the fibrils observed in samples that had been incubated for 48 h appeared to be longer and slightly less prevalent, although they were still abundant.

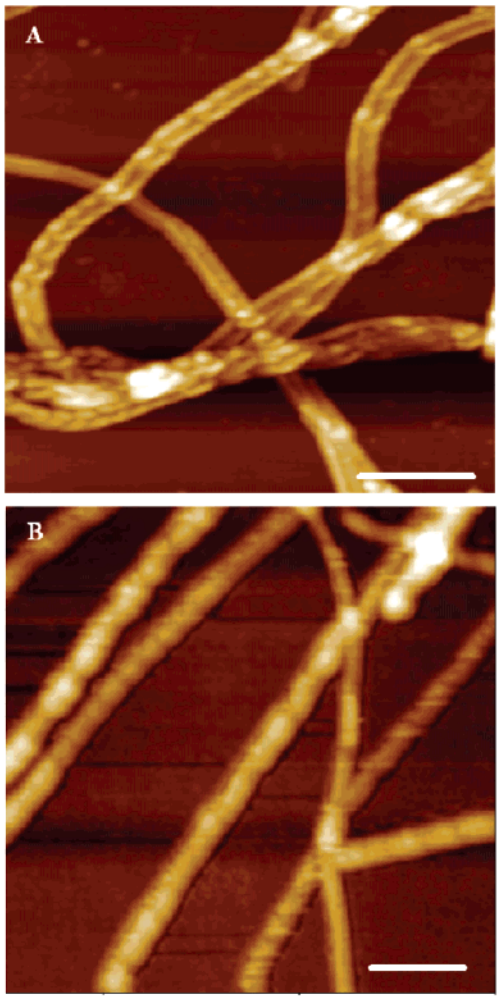

FIGURE 5: IAPP-3XL forms amyloid deposits. Tapping mode AFM images of (A) wild-type human IAPP and (B) the IAPP-3XL mutant. The horizontal scale bar represents 250 (A) and 200 nm (B). The vertical *Z* scale is 60 (A) and 20 nm (B). Fibrils were prepared at pH 7.4 and 25 °C in 20 mM Tris-HCl and 2% HFIP (v/v), yielding 0.14 mg/mL peptide.

We also used atomic force microscopy (AFM) to examine the topology of the fibrils formed by the 3XL mutant. Tapping mode AFM has been used to probe the morphology of amyloid fibrils formed by a wide range of proteins and polypeptides and is a technique that complements TEM, since samples do not have to be either stained with heavy metal or visualized under high-vacuum conditions. Our ambient AFM data are consistent with the TEM studies and support the conclusion that the triple leucine mutant forms amyloid fibrils. Figure 5 compares AFM images of wild-type IAPP and IAPP-3XL, both of which formed left-handed helical, slightly curved fibrils. The images are broadly similar and reveal features typically observed for AFM images of amyloid fibrils, including the same sense of the helical twist. There are differences in the details of the images, however. For example, the twisted ribbon morphology was noticeably more pronounced for the wild-type fibrils. A distinct periodicity is observed for both peptides which is typical of amyloid. For the wild-type IAPP fibril, the period is 47.2 $\pm$ 9.0 nm, whereas for the IAPP-3XL mutant, the period is 62.1 $\pm$ 8.5 nm, indicative of observable macroscopic changes in the fibril structure which result from differences in the two peptide sequences. A similar argument has been previ-

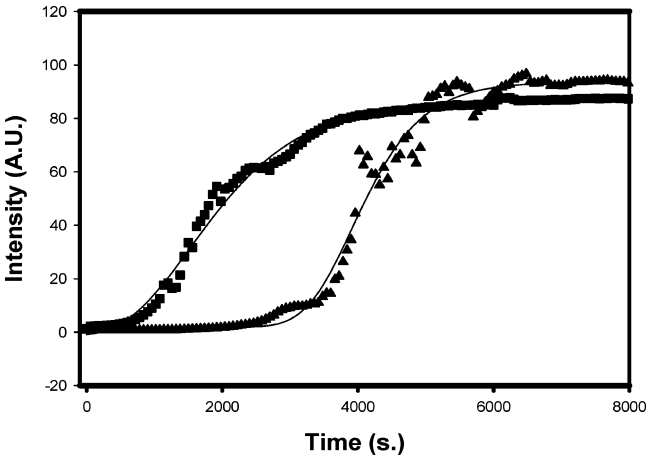

FIGURE 6: IAPP-3XL forms amyloid significantly more slowly than wild-type IAPP. Thioflavin fluorescence monitored kinetic assays of fibril formation by wild-type IAPP and IAPP-3XL. Reactions were initiated by diluting HFIP stock solutions into aqueous buffer. Final conditions were 32 μM thioflavin-T, 17 mM Tris-HCl (pH 7.4), and 0.14 mg/mL peptide. Experiments were performed with continuous stirring at 25 °C. The solid line represents the best fit to a sigmoidal curve.

ously advanced to explain polymorphic fibrillar morphologies (*28*, *29*). The distribution of fibril lengths is similar for the two peptides in the sense of ranging from 100 nm to several micrometers. However, there are differences in the distribution of heights worth discussing (Supporting Information).

The mean height for the wild-type peptide is 5.16 ± 1.46 nm, and the median is 4.71 nm. The measured fibril height is within the range expected and is in agreement with previous AFM data as well as electron microscopy results for human IAPP (*30*−*33*). Nonetheless, as seen in Figure 5, the wild-type fibrils tend to occur mainly as pairs of fibrils and sometimes as triplets and multiplets of adjoining fibrillar structures. This result is consistent with a picture of wild-type fibrils being composed of laterally intertwined component fibrillar building blocks forming higher-order structures and, moreover, argues for the reasonable hypothesis that the aromatic residues help to mediate interfibril interactions. Our observation is also in agreement with previous reports on IAPP assemblies, where fibril structures were observed (*34*). In other words, it is plausible that the aromatic residues, through favorable π-stacking interactions or aromatic hydrophobic interactions, may encourage formation of a hierarchical fibrillar architecture. By contrast, the mean height for fibrils formed by the 3XL mutant, 3.39 ± 1.3 nm, is clearly shorter than that of the wild type, as is the median height, 3.1 nm. This may result from an unfavorable tendency for component fibrils to aggregate in this system as compared with that of the wild type.

The results of these experiments are all internally consistent and demonstrate that interactions involving aromatic residues are not required for amyloid formation by IAPP. However, these studies do not address whether aromatic−aromatic or aromatic−hydrophobic interactions influence the rate of assembly of IAPP fibrils. Consequently, we conducted kinetic assays to compare the rate of amyloid formation by wild-type IAPP and the 3XL mutant. Figure 6 compares the time course of fibril formation as monitored by thioflavin-T binding. Both the wild-type and 3XL peptides exhibit a lag phase with little or no change in fluorescence followed by a rapid growth phase leading to the final plateau. The lag phase is noticeably longer for the 3XL mutant, increasing by a factor of approximately 5. Interestingly, the effect on the growth phase is less pronounced.

CONCLUSIONS

Spectroscopy measurements and TEM and AFM studies of IAPP-3XL clearly demonstrate that it readily aggregates into fibrils that bind thioflavin-T, have considerable β-sheet structure, and have the morphology expected for amyloid deposits. These studies unequivocally show that IAPP-3XL forms amyloid despite the complete absence of aromatic residues. We believe that our observations with full-length IAPP are important because previous studies of the role of aromatic residues in fibril formation by IAPP involved studies of short peptides which contained only a single aromatic amino acid. In contrast, mature IAPP contains three aromatic residues, and aromatic contacts are known to be formed during the fibrillization process (*14*). Thus, the study presented here extends our earlier observations by showing that intrapeptide aromatic−aromatic interactions are not required for fibril formation. This study together with recent studies of the role of aromatic interactions in amyloid formation by muscle acylphosphatase and prior investigations of short peptides clearly demonstrate that aromatic−aromatic or aromatic−hydrophobic interactions are not a requirement for amyloid formation in all systems (*2*, *13*). Our kinetic studies, however, do show that interactions involving aromatic residues of IAPP are important during the lag phase, and our AFM measurements show that they influence the morphology of the deposits.

It is interesting to speculate about the molecular basis for the elongation of the lag phase caused by the aromatic to leucine substitutions. In principle, the substitutions could modulate conformational tendencies and fluctuations within the monomeric ensemble, or they might destabilize specific intramolecular contacts or modulate important peptide−peptide interactions. Of course, the substitutions could exert their net effect by some combination of these processes, although it is very difficult to quantify or differentiate these potential multiple effects. There are literature data, however, which suggest that at least part of the effects could be due to modulation of intramolecular aromatic−aromatic interactions. In particular, FRET-based measurements showed that aromatic residues in wild-type IAPP form interactions during the lag phase of amyloid formation and demonstrated that the C-terminal tyrosine makes contacts with one or more of the phenylalanines (*14*). Our study complements this investigation by showing that these interactions are likely to be kinetically important. These observations are important for mechanistic interpretation of amyloid fibril assembly of IAPP and may be relevant for the design of inhibitors of aggregation (*15*, *16*, *25*).

Might aromatic−aromatic interactions be important in in vivo amyloid formation by IAPP? It can be very difficult to extrapolate effects observed in in vitro biophysical studies to in vivo amyloid formation in the complicated extracellular environment. In vivo amyloid formation is a dynamic process involving amyloid deposition, potential disruption of amyloid deposits, and interactions with cellular quality control machinery. If the 5-fold increase in the lag phase were

translated into the in vivo environment, then the effects might indeed be significant and replacement of the aromatic residue in IAPP might decrease the level of amyloid formation. Conversely, the aromatic residues in IAPP might actually inhibit amyloid formation by modulating interactions between IAPP and other molecules, and their removal could then be deleterious. In particular, aromatic residues in IAPP have been implicated in IAPP−insulin interactions (*35*). This is potentially greatly important because insulin is a potent inhibitor of amyloid formation by IAPP in vitro, and there has been speculation that this could be relevant in vivo (*36*−*38*). The concentration of IAPP in the secretory granule is well above concentrations that lead to rapid aggregation in vitro, leading to the question of why amyloid formation is inhibited in the granule. Insulin−IAPP interactions have been proposed to be the key. Thus, disruption of the insulin−IAPP interaction by replacement of the aromatic residues might promote amyloid formation.

In summary, our studies demonstrate that intramolecular or intermolecular aromatic−aromatic or aromatic−hydrophobic interactions are not required for amyloid formation by IAPP. However, the data presented here clearly support a role for aromatic residues in the kinetics of amyloid assembly and show that they influence the morphology of the deposits.

SUPPORTING INFORMATION AVAILABLE

Two plots showing histograms of the height distributions of wild-type amyloid fibrils and of amyloid fibrils formed by the 3XL mutant, as determined by AFM. This material is available free of charge via the Internet at http://pubs.acs.org.

REFERENCES

1. Gazit, E. (2002) A possible role for π-stacking in the self-assembly of amyloid fibrils, *FASEB J. 16*, 77−83.
2. Bemporad, F., Taddei, N., Stefani, M., and Chiti, F. (2006) Assessing the role of aromatic residues in the amyloid aggregation of human muscle acylphosphatase, *Protein Sci. 15*, 852−870.
3. Jack, E., Newsome, M., Stockley, P., Radford, S., and Middleton, D. (2006) The organization of aromatic side groups in an amyloid fibril probed by solid-state ^{2}H and ^{19}F NMR spectroscopy, *J. Am. Chem. Soc. 128*, 8098−8099.
4. Kapurniotu, A. (2001) Amyloidogenicity and cytotoxicity of islet amyloid polypeptide, *Pept. Sci. 60*, 438−459.
5. Zanuy, D., Porat, Y., Gazit, E., and Nussinov, R. (2004) Peptide sequence and amyloid formation: Molecular simulations and experimental study of a human islet amyloid polypeptide fragment and its analogs, *Structure 12*, 439−455.
6. Tartaglia, G. G., Cavalli, A., Pellarin, R., and Caflisch, A. (2004) The role of aromaticity, exposed surface and dipole moment in determing protein aggregation rates, *Protein Sci. 13*, 1939−1941.
7. Yoon, S., and Welsh, W. J. (2004) Detecting hidden sequence propensity for amyloid fibril formation, *Protein Sci. 13*, 2149−2160.
8. Bemporad, F., Calloni, G., Campioni, S., Plakoutsi, G., Taddel, N., and Chiti, F. (2006) Sequence and structural determinations of amyloid fibril formation, *Acc. Chem. Res. 39*, 620−627.
9. Chiti, F., Stefani, M., Taddei, N., Ramponi, G., and Dobson, C. M. (2003) Rationalization of the effects of mutations on peptide and protein aggregation, *Nature 424*, 805−809.
10. Ferandez-Escamilla, A. M., Rousseau, F., Schymkowitz, J., and Serrano, L. (2004) Predication of sequence-dependent and mutational effects on the aggregation of peptide and proteins, *Nat. Biotechnol. 22*, 1302−1306.
11. Burley, S. K., and Petsko, G. A. (1988) Weakly polar interactions in proteins, *Adv. Protein Chem. 39*, 125−189.
12. Azriel, R., and Gazit, E. (2001) Analysis of the minimal amyloid-forming fragment of the islet amyloid polypeptide, *J. Biol. Chem. 276*, 34156−34161.
13. Tracz, S., Abedini, A., Driscoll, M., and Raleigh, D. (2004) Role of aromatic interactions in amyloid formation by peptides derived from human amylin, *Biochemistry 43*, 15901−15908.
14. Padrick, S., and Miranker, A. (2001) Islet amylyoid polypeptide: Identification of long-range contacts and local order on the fibrillogenesis pathway, *J. Mol. Biol. 308*, 783−794.
15. Porat, Y., Mazor, Y., Efrat, S., and Gazit, E. (2004) Inhibition of islet amyloid polypeptide fibril formation: A potential role for heteroaromatic interactions, *Biochemistry 43*, 14454−14462.
16. Porat, Y., Abramowitz, A., and Gazit, E. (2006) Inhibition of amyloid fibril formation by polyphenols: Structural similarity and aromatic interactions as a common inhibition mechanism, *Chem. Biol. Drug Des. 67*, 27−37.
17. Cooper, G. J. S., Willis, A. C., Clark, A., Turner, R. C., Sim, R. B., and Reid, K. B. M. (1987) Purification and characterization of a peptide from amyloid rich pancreases of type II diabetic patients, *Proc. Natl. Acad. Sci. U.S.A. 84*, 8628−8632.
18. Westermark, P., Wernstedt, C., Wilander, E., Hayden, D. W., O'Brien, T. D., and Johnson, K. H. (1987) Amyloid fibrils in human insulinoma and islets of langerhans of the diabetic cat are derived from a neuropeptide-like protein also present in normal islet cells, *Proc. Natl. Acad. Sci. U.S.A. 84*, 3881−3885.
19. Clark, A., Wells, C. A., Buley, I. D., Cruickshank, J. K., Vanhegan, R. I., Matthews, D. R., Cooper, G. J., Holman, R. R., and Turner, R. C. (1988) Islet amyloid, increased A-cells, reduced B-cells and exocrine fibrosis: Quantitative changes in the pancreas in type 2 diabetes, *Diabetes Res. Clin. Pract. 9*, 151−159.
20. Kahn, S. E., D'Alessio, D. A., Schwartz, M. W., Fujimoto, W. Y., Ensinck, J. W., Taborsky, G. J. J., and Porte, D. J. (1990) Evidence of cosecretion of islet amyloid polypeptide and insulin by β-cells, *Diabetes 39*, 634−638.
21. Kahn, S. E., Andrikopoulos, S., and Verchere, C. B. (1999) Islet amyloid: A long-recognized but underappreciated pathological feature of type 2 diabetes, *Diabetes 48*, 241−253.
22. Jaikaran, E., and Clark, A. (2001) Islet amyloid and type 2 diabetes: From molecular misfolding to islet pathophysiology, *Biochim. Biophys. Acta 1537*, 179−203.
23. Clark, A., Lewis, C. E., Willis, A. C., Cooper, G. J. S., Morris, J. F., Reid, K. B. M., and Turner, R. C. (1987) Islet amyloid formed from diabetes-associated peptide may be pathogenic in type-2 diabetes, *Lancet 2*, 231−234.
24. Kajava, A. V., Aebi, U., and Steven, A. C. (2005) The parallel superpleated β-structure as a model for amyloid fibrils of human amylin, *J. Mol. Biol. 348*, 247−252.
25. Gazit, E. (2002) Mechanistic studies of the process of amyloid fibrils formation by the use of peptide fragments and analogues: Implications for the design of fibrillization inhibitors, *Curr. Med. Chem. 9*, 1725−1735.
26. Abedini, A., and Raleigh, D. P. (2005) Incorporation of pseudoproline derivatives allow the facile synthesis of human IAPP: A highly amyloidogenic and aggregation-prone polypeptide, *Org. Lett. 7*, 693−696.
27. Abedini, A., and Raleigh, D. (2005) The role of His-18 in amyloid formation by human islet amyloid polypeptide, *Biochemistry 44*, 16284−16291.
28. Lashuel, H. A., LaBrenz, S. R., Woo, L., Serpell, L. C., and Kelly, J. W. (2000) Protofilaments, filaments, ribbons, and fibrils from peptidomimetic self-assembly: Implications for amyloid fibril formation and materials science, *J. Am. Chem. Soc. 122*, 5262−5277.
29. Tenidis, K., Waldner, M., Bernhagen, J., Fischle, W., Bergmann, M., Weber, M., Merkle, M.-L., Voelter, W., Brunner, H., and Kapurniotu, A. (2000) Identification of a penta- and hexapeptide of islet amyloid polypeptide (IAPP) with amyloidogenic and cytotoxic properties, *J. Mol. Biol. 295*, 1055−1071.
30. Green, J. D., Goldsbury, C., Kistler, J., Cooper, G. J. S., and Aebi, U. (2004) Human amylin oligomer growth and fibril elongation define two distinct phases in amyloid formation, *J. Biol. Chem. 279*, 12206−12212.
31. Goldsbury, C., Kistler, J., Aebi, U., Arvinte, T., and Cooper, G. J. S. (1999) Watching amyloid fibrils grow by time-lapse atomic force microscopy, *J. Mol. Biol. 285*, 33−39.
32. Kayed, R., Bernhagen, J., Greenfield, N., Sweimeh, K., Brunner, H., Voelter, W., and Kapurniotu, A. (1999) Conformational transitions of islet amyloid polypeptide (IAPP) in amyloid formation in vitro, *J. Mol. Biol. 287*, 781−796.

33. Goldsbury, C. S., Cooper, G. J. S., Goldie, K. N., Muller, S. A., Saafi, E. L., Gruijters, W. T. M., Misur, M. P., Engel, A., Aebi, U., and Kistler, J. (1997) Polymorphic fibrillar assembly of human amylin, *J. Struct. Biol. 119*, 17−27.
34. Sedman, V. L., Allen, S., Chan, W. C., Davies, M. C., Roberts, C. J., and Tendler, S. J. B. (2005) Atomic force microscopy of human amylin (20−29) fibrils, *Protein Pept. Lett. 12*, 79−83.
35. Gilead, S., Wolfenson, H., and Gazit, E. (2006) Molecular mapping of the recognition interface between the islet amyloid polypeptide and insulin, *Angew. Chem., Int. Ed. 45*, 6476−6480.
36. Westermark, P., Li, Z. C., Westermark, G. T., Leckstrom, A., and Steiner, D. F. (1996) Effects of β cell granule components on human islet amyloid polypeptide fibril formation, *FEBS Lett. 379*, 203−206.
37. Kudva, Y. C., Mueske, C., Butler, P. C., and Eberhardt, N. L. (1998) A novel assay in vitro of human islet amyloid polypeptide amyloidogenesis and effects of insulin secretory vesicle peptides on amyloid formation, *Biochem. J. 331*, 809−813.
38. Larson, J. L., and Miranker, A. D. (2004) The mechanism of insulin action on islet amyloid polypeptide fiber formation, *J. Mol. Biol. 335*, 221−231.
39. Jaikaran, N. T., Nilsson, M. R., and Clark, A. (2004) Pancreatic β-cell granule peptides form heteromolecular complexes which inhibit islet amyloid polypeptide fibril formation, *Biochem. J. 377*, 709−716.

BI0621967